

# GPOpt: Teaching LLMs to do Interpretable Black-Box Optimization

Jamison Meindl <sup>\*1</sup> Yunsheng Tian <sup>1</sup> Tony Cui <sup>1</sup> Veronika Thost <sup>2</sup> Zhang-Wei Hong <sup>2</sup> Jie Chen <sup>2</sup>  
Wojciech Matusik <sup>1</sup> Mina Konaković Luković <sup>1</sup>

## Abstract

Global optimization of expensive, derivative-free black-box functions demands extreme sample efficiency and decision interpretability. While Large Language Models (LLMs) have shown broad capabilities, even state-of-the-art models remain limited in solving continuous black-box optimization tasks and struggle to maintain exploration-exploitation balance. We introduce GPOpt, an optimization method that equips LLMs with continuous black-box optimization capabilities by fine-tuning Llama 3.1 8B on structured Bayesian optimization (BO) data, including surrogate model information. This provides an explainable framework calibrated to produce surrogate model outputs comparable to a Gaussian process, while keeping the advantages of flexible LLM-based optimization. On a variety of black-box optimization benchmarks, our model shows favorable performance compared to traditional optimizers and transformer-based alternatives, while providing important context and insight into the model’s decisions.

## 1. Introduction

Black-box optimization under tight evaluation budgets is pivotal in many scientific and engineering settings. Practitioners frequently utilize gradient-free heuristics such as genetic algorithms (Holland, 1992), simulated annealing (Kirkpatrick et al., 1983), and evolutionary strategies (Hansen & Ostermeier, 2001), which often require thousands of evaluations to converge. When each experiment or simulation is slow or costly, such sample counts become prohibitive. Therefore, we focus on improving continuous black-box optimization under strict evaluation budgets.

To illustrate this problem, consider a self-driving laboratory that optimizes the yield of a complex chemical synthesis. The process is governed by continuous parameters such as

<sup>1</sup>MIT <sup>2</sup>MIT-IBM Watson AI Lab. Correspondence to: Jamison Meindl <jmeindl@mit.edu>.

temperature, pressure, and catalyst concentration, but the precise relationship between these inputs and the reaction yield is unknown and non-differentiable. Each experiment consumes expensive reagents and occupies physical equipment for hours, strictly limiting the budget to a small number of trials (e.g.,  $N < 50$ ). Consequently, the optimizer must strategically select the next experimental conditions, balancing the exploration of the parameter space with the exploitation of conditions already known to be effective. Developing an optimizer with better performance than the existing methods provides a valuable opportunity to solve these problems more efficiently.

One of the most efficient approaches to solving such problems is Bayesian optimization (BO) (Shahriari et al., 2015), which performs effective optimization by fitting a probabilistic surrogate, typically a Gaussian process, and selecting queries via a heuristic acquisition function that balances exploration and exploitation. BO has driven progress in materials discovery (Erps et al., 2021), molecular design (Griffiths & Hernández-Lobato, 2020), clinical prognosis (Alaa & Schaar, 2018), and hyperparameter tuning (Turner et al., 2021). BO has proven to be a robust method in these real-world fields and therefore is a valuable source of data and inspiration for learned optimization methods.

**Regime of Interest:** We consider the black-box global optimization problem  $\mathbf{x}^* = \arg \min_{\mathbf{x} \in \mathcal{X}} f(\mathbf{x})$ , where  $\mathbf{x} \in \mathbb{R}^d$  denotes the decision variables. The feasible search space  $\mathcal{X}$  is a  $d$ -dimensional hyper-rectangle defined by box constraints, such that  $\mathcal{X} = \{\mathbf{x} \in \mathbb{R}^d \mid l_i \leq x_i \leq u_i, \forall i = 1, \dots, d\}$ , with fixed bounds  $\mathbf{l}, \mathbf{u} \in \mathbb{R}^d$ . The objective function  $f : \mathcal{X} \rightarrow \mathbb{R}$  is treated as a black box; it is computationally expensive to evaluate and gradient-free. Our focus is strictly on the continuous low-dimensional, ultra-low budget regime. We address problems with dimensionality  $d \leq 10$  and a total evaluation budget limited to  $N \leq 50$  evaluations. However, our methodology is scalable to broader domains and is not inherently limited to this scope. This regime still captures experimental problems where the evaluations are limited by risk, availability, or cost. Relevant domains include particle accelerator tuning (Shalloo et al., 2020), robotic control (Calandra et al., 2016), and battery optimization (Attia et al., 2020), as well as many other fields.

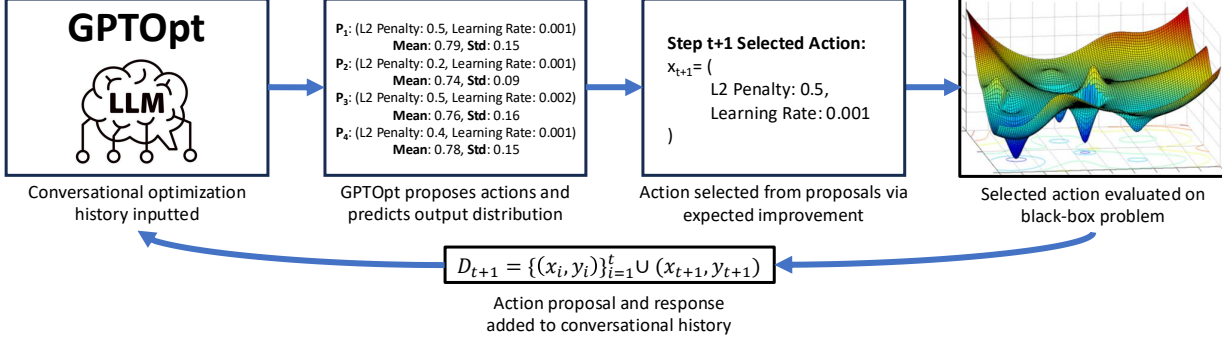


Figure 1. Overall diagram of GPTOpt. This describes the inference usage of GPTOpt for a real-world black-box optimization problem.

**Motivation:** While BO provides an understandable backbone for its decision process in its surrogate model, generally a Gaussian process, LLM-based methods are more difficult to interpret and generally do not have this verifiable aspect of their decision process. When tested on problems without rich semantic priors, state-of-the-art LLMs struggle to accurately model the function space, particularly the uncertainty of the surrogate model, and therefore fail to solve complex optimization problems (Huang et al., 2024). However, due to their vast knowledge base, LLMs have been shown to act as a high-quality surrogate model when given additional semantic information about the black-box problem (Liu et al., 2024). At the same time, small transformer-based models have been shown to accurately model Gaussian process (GP) surrogate models by training on surrogate model data in PFNs4BO (Müller et al., 2023). However, using this methodology on an LLM would be very computationally expensive, as thousands of inference passes would be needed for each parameter selection.

Therefore, creating a model that has both of these advantages, being a reliable surrogate model when information is sparse, and the ability to utilize a vast knowledge base to improve optimization would bridge this gap in LLM optimization performance. To achieve this, we propose a data generation and fine-tuning methodology heavily linked to BO and GPs that augments LLMs with accurate surrogate modeling capability and improved black-box optimization performance. By combining learning on high-quality BO trajectories with learning a GP surrogate, we wish to demonstrate that these two paradigms can be combined to create an interpretable LLM-based black-box optimization assistant.

Our key contributions are as follows:

1. We develop a diverse synthetic function generator and compile 2,000,000 optimization trajectories generated with BO to be used as fine-tuning data.
2. We design a structured fine-tuning approach that teaches LLMs to act like Gaussian process surrogate

models generated during successful BO trajectories.

3. We demonstrate that our LLM-based model iteratively updates a calibrated understanding of the function space similar to a Gaussian process.
4. Our evaluation demonstrates favorable performance compared to traditional optimizers and state-of-the-art LLMs across a variety of continuous black-box optimization benchmarks.

## 2. Related Work

**Bayesian Optimization (BO):** BO is a powerful global optimization technique due to its ability to efficiently handle expensive black-box functions by balancing exploration and exploitation with carefully designed acquisition functions, such as Expected Improvement (EI), LogEI (Ament et al., 2023), and Upper Confidence Bound (UCB). Designed with different principles of trading off exploration and exploitation, they suit different types of optimization problems. BO has been made accessible by a collection of open-source libraries and software including Spearmint (Snoek et al., 2012), BoTorch (Balandat et al., 2020), AutoOED (Tian et al., 2021), SMAC3 (Lindauer et al., 2022), HEBO (Cowen-Rivers et al., 2022a), Openbox (Jiang et al., 2024), and Vizier (Golovin et al., 2017; Song et al., 2024b). However, it remains a challenge for users to determine the most appropriate configuration for their specific problem setting, as the selection is often heuristic and depends on the problem landscape.

**Learning to Optimize:** The evolution of learned black-box optimization has transitioned from early RNN-based sequence prediction (Li & Malik, 2016; Andrychowicz et al., 2016) toward advanced transformer-based frameworks that leverage increased computational capabilities. While initial transformer applications like MELBA (Chayboubi et al., 2022) and Neural Acquisition Process (Maraval et al., 2024) utilized online RL for task-specific solvers,

and POM (Li et al., 2024) focused on high-dimensional evolutionary strategies, recent work aims for broader generalization in black-box settings. Significant developments include PFNs4BO (Müller et al., 2023), which uses prior-data fitted networks to mimic surrogate models for general-purpose optimization, and BONET (Krishnamoorthy et al., 2022), which applies causal transformers to optimization trajectories. OptFormer (Chen et al., 2022) demonstrates the potential of training text-based transformers on large proprietary datasets, while RIBBO (Song et al., 2024a) utilizes offline reinforcement learning with conditional rewards to outperform the underlying training data distributions. Lastly, ZeroShotOpt (Meindl et al., 2025) demonstrates that transformer-based models can learn to model BO trajectories when trained on large-scale synthetic functions. These methods represent a wide range of transformer-based training mechanisms that show that training on large-scale datasets can yield strong optimization generalization.

**LLM-based Optimization:** Large language models have also been applied out of the box for black-box optimization. LLAMBO (Liu et al., 2024), Reasoning BO (Yang et al., 2025), and EvoLLM (Lange et al., 2024) demonstrate that effective prompting techniques and contextual information combined with LLMs can yield high-quality optimization trajectories. These methods highlight the potential of LLMs to iteratively improve black-box optimization objectives, especially when combined with semantic information, but lack the understandability and verification of the decision process that comes with statistical methods, including BO. Additionally, Huang et al. (2024) show that current LLMs are not capable of performing advanced black-box optimization without knowledge of the function space. Their experiments on a variety of state-of-the-art models show that LLMs can do some basic black-box optimization tasks, but fail to match the performance of BO.

With GPTOpt, we provide a data generation and LLM fine-tuning framework integrated with Gaussian processes and Bayesian optimization. By providing the model with high-quality trajectories generated by BO and contextualizing with the predicted distribution provided by GPs, we aim to construct a more robust and interpretable LLM-based optimization framework.

### 3. Methodology

**Problem Framing:** We frame the optimization as a sequential decision-making process via multi-turn LLM prompts. The LLM acts as an agent interacting with the function  $f$  over discrete steps  $t = 1, \dots, N$ . At step  $t$ , the agent observes the history of past evaluations  $\mathcal{D}_t = \{(\mathbf{x}_i, y_i)\}_{i=1}^t$ , where  $y_i = f(\mathbf{x}_i)$ . Based on  $\mathcal{D}_t$ , the agent selects the next query point  $\mathbf{x}_{t+1}$ . This cycle repeats until the bud-

get  $N$  is exhausted. The goal is to find an optimizer  $\hat{\mathbf{x}} \in \{\mathbf{x}_1, \dots, \mathbf{x}_N\}$  such that  $f(\hat{\mathbf{x}})$  is close to  $f(\mathbf{x}^*)$ .

#### 3.1. Dataset Generation

**Synthetic Dataset:** Due to the lack of widely available real-world test functions, we aim to create realistic and diverse synthetic functions to compile a large-scale dataset for model fine-tuning. To do this, we use Gaussian Processes (GPs) as flexible function generators, which allows for large-scale data collection and realistic landscapes. The intuition here is that GP-based BO methods perform well over a wide variety of function spaces, so by basing our training data on GP functions as well, we hope to learn a policy that also adapts well to various function spaces. To further diversify our training dataset, we vary the scale of input and output parameters to various realistic regimes. For example, we include objectives in  $[0, 100]$  or  $[1, 10]$  and parameters in  $[0, 1]$  or  $[0.0001, 0.1]$ . We randomly generate a large number of random scales to allow for generalization. We also add further augmentations to the randomly generated GP process. These augmentations transform smooth GP samples into challenging, realistic landscapes by applying non-linear coordinate warping, introducing discontinuities, and adding constraints. The goal of this process is to create a training set that mimics the irregularity of real-world systems. By creating functions with these diverse methods, we provide a base for the model to learn realistic function dynamics across a variety of possible function spaces.

**BO Data:** We choose to train our model on successful optimization examples, using BO with 10 acquisition function variants as our expert to generate trajectories on our synthetic functions. These include LogEI (Ament et al., 2023), Upper Confidence Bound (UCB), and Probability of Improvement (PI), each with varying exploration-exploitation parameters. Specifically, we adapt the acquisition parameters for LogEI and PI across a range of 3 values, and for UCB across a range of 4 values. We generate 10,000 synthetic functions for each dimension ranging from 2D to 10D for both GP and augmented GP function spaces, totaling 20,000 functions per dimension. To compile our training dataset, we select the best trajectory from among the acquisition functions at fixed lengths of 10, 25, and 50 total evaluations. This results in over 500,000 trajectories. We further augment this by flipping the axes, flipping the action space, and randomizing initial point order to expand the overall quantity of data to around 2 million total trajectories.

**Prompt Structure:** An example of the interaction loop is shown in Figure 2. The prompt begins with a system instruction defining the agent’s role as a black-box optimization assistant and enforcing a strict JSON output format containing the action and predicted mean and standard devi-

```

System: You are a black-box optimization assistant. Your goal is to iteratively select new points to maximize the objective within 10 total evaluations. You must output the raw parameter values within the specified ranges as well as a predicted mean and standard deviation for the selected point.
Output exactly ONE valid JSON object containing the "Action", "Mean", and "Std", with no surrounding text.
User: Problem description: This problem is a synthetic 3D black-box optimization problem.
The JSON must have exactly these keys: {"Action": {...}, "Mean": <float>, "Std": <float>}
We have collected 5 random initial points:
{"Step": 1, "Action": {"param_0": 0.406, "param_1": 0.31867, "param_2": 0.00536228}, "Evaluated Objective": 660479}
... [Steps 2-4 omitted] ...
{"Step": 5, "Action": {"param_0": 0.353, "param_1": 0.602819, "param_2": 0.112898}, "Evaluated Objective": 650711}
Based on the history, iteratively generate the next configuration to maximize the objective. You have 5 evaluations left.
Assistant: {"Action": {"param_0": 0.173, "param_1": 0.322, "param_2": 0.0002}, "Mean": 658314, "Std": 7094}
User: {"Step": 6, "Evaluated Objective": 651697}
Assistant: {"Action": {"param_0": 0.423, "param_1": 0.274, "param_2": 0.1323}, "Mean": 658769, "Std": 5029}
... [Steps 7-10 omitted] ...

```

Figure 2. Example interaction loop. The system instructions are provided, while the interaction history is abbreviated for space.

ation. The user then provides the problem description and the randomly initialized points. We provide all numbers rounded to 6 significant figures and convert the BO steps into a multi-turn user and assistant conversation. The interaction follows in a turn-based manner where the assistant proposes a new configuration, which is the action proposed by BO and the GP’s predicted mean and standard deviation, and the user returns the evaluated objective value, repeating until the evaluation budget is exhausted.

**GP Posterior:** The “Mean” and “Std” values correspond to the posterior of a Gaussian Process (GP) surrogate used in BO. Given a history of observations  $\mathcal{D}_t = \{(\mathbf{x}_i, y_i)\}_{i=1}^t$ , the posterior distribution at a new candidate point  $\mathbf{x}$  is modeled as a Gaussian:  $P(f(\mathbf{x}) | \mathcal{D}_t) = \mathcal{N}(\mu(\mathbf{x}), \sigma^2(\mathbf{x}))$ . In this context,  $\mu(\mathbf{x})$  acts as the surrogate prediction for the objective function, while  $\sigma(\mathbf{x})$  quantifies the uncertainty in that region of the search space.

**Learning Objective:** We aim to train the model to accurately predict these GP posterior statistics directly from the interaction history. By supervising the model to predict the GP’s  $\mu(\mathbf{x})$  and  $\sigma(\mathbf{x})$  for each action selected by BO, the model learns a probabilistic representation of the optimization landscape. This explicitly aligns the language model’s reasoning with the mechanics of GPs, such that its proposals are not just heuristic guesses but are grounded in a calibrated estimate of the optimization landscape.

**Real-world Context and Explanations:** To further expand the capabilities of our model, we augment our synthetic dataset with two types of LLM-generated descriptions. First, we generate descriptions of real-world problems, including descriptions of the overall problem, the parameters to optimize, and the evaluation metric. This associates the model with diverse and realistic descriptions that the model can use as semantic information for real-world experiments. Additionally, we augment a portion of our dataset with LLM-generated explanations for each action selection, as

shown by the example in Figure 3. The real-world context or explanations are included for around 1% of our overall dataset. We provide more detail about how these samples are generated in Appendix A.3.

```

Assistant: {
  "Action": {
    "outlet_line_length_m": 18.1777,
    "pulsation_damper_volume_L": 15.2838,
    "discharge_throttle_percent": 55.1114,
    "pump_speed_rpm": 1913.44
  },
  "Mean": 4.53466,
  "Std": 0.204994,
  "Explanation": "I proposed a candidate at long length with high throttle and moderate damper to follow up on an observed improvement when throttle was increased in that regime. This action leans toward exploitation of the promising long-length/high-throttle region while still retaining diversity in damper size. The choice aims to confirm whether high throttle is consistently beneficial with different damper volumes."
}
User: {"Step": 13, "Evaluated Objective": 2.71392}

```

Figure 3. Example of an augmented interaction step with real-world context within the training data. The data includes the step’s selected action, GP posterior predictions, and a natural language explanation justifying the strategy.

### 3.2. Training

Our experiments utilize Llama 3.1 8B Instruct (Dubey et al., 2024) as the base model. We chose this model for its balance of instruction-following ability and computational accessibility. Fine-tuning is performed via Low-Rank Adaptation (LoRA) (Hu et al., 2022) leveraging the Unslloth framework (Daniel Han & team, 2023), which significantly optimizes training throughput on limited hardware. We use LoRA fine-tuning to allow the model to maintain its knowledge base while adding the ability to model BO trajectories.

We fine-tune the model with a batch size of 128 trajectories for one epoch on our dataset of 2 million BO trajectories. These trajectories are provided in the text form shown in

Figure 2 and trained via supervised next-token prediction on the assistant portions only. This training takes around 7 days on two NVIDIA H200 GPUs. Additional implementation details and hyperparameters are provided in Appendix A.4.

### 3.3. Inference

At inference time, we utilize the results of our surrogate model predictions to improve the exploration-exploitation balance of our selections, similar to OptFormer (Chen et al., 2022). We do this by prompting the model  $k$  times at each step, resulting in  $k$  proposed actions and associated predicted distributions. We then calculate the expected improvement using the predicted distributions and select the proposed action with the highest expected improvement relative to the previous best value. We find that  $k = 4$ , with a sampling temperature of 1.5 and a top-p value of 0.95, yields the best results. We provide ablations for these selections in Section 4.6 and use these parameters in our experiments.

## 4. Results

### 4.1. Benchmark Performance

We test our methodology on a variety of out-of-distribution black-box optimization benchmarks. We test on standard black-box optimization benchmarks to evaluate model performance without semantic priors, which demonstrates the challenges that other LLM-based optimization methods face. We include optimization benchmarks in 2D, 5D, and 10D from the Black-Box Optimization Benchmark (BBOB) (El-hara et al., 2019) and the Virtual Library of Simulated Experiments (VLSE) (Surjanovic & Bingham, 2013). These both contain functions that are traditionally used as standard benchmarks for global black-box optimization.

We compare GPOpt against a comprehensive set of baselines, including classical optimizers, state-of-the-art Bayesian Optimization (BO) approaches, and emerging transformer-based methods. We utilize implementations from Optuna (Akiba et al., 2019) and OptunaHub (Ozaki et al., 2025) for the following primary baselines:

- **Classical & BO:** CMA-ES (Hansen et al., 2003), HEBO (Cowen-Rivers et al., 2022b), TuRBO (Eriksson et al., 2019), AutoSampler, TPE, SMAC (Lindauer et al., 2022), BoTorch (Balandat et al., 2020), PSO (Kennedy & Eberhart, 1995), and Differential Evolution (Lampinen & Storn, 2004).
- **Transformer-based:** LLAMBO (Liu et al., 2024) and PFNs4BO (Müller et al., 2023).

To isolate the impact of our fine-tuning, we also evaluate the base Llama 3.1 8B Instruct model (Dubey et al., 2024) and

OpenAI GPT-5 (Singh et al., 2025) using the same prompts as GPOpt. As a whole, these methods represent the current state-of-the-art in classical optimization and the latest developments in learned optimization. For all experiments, we use the default parameters provided in OptunaHub.

We show the performance of each method on these benchmarks using mean normalized performance. Normalized performance evaluates the performance of each method in relation to the overall optimality gap while factoring in the scale of the function. We measure this with the following:

$$P = 1 - (|f_{\text{best}} - f^*| / |f_m - f^*|)$$

where  $f_{\text{best}}$  is the best sampled value,  $f^*$  is the global optimum, and  $f_m$  is the median of randomly sampled points. We report the mean performance over the tested functions and show the step progression up to the final steps.

We show the performance of GPOpt on the BBOB test suite in Figure 4 and the VLSE test suite in Figure 5. We see that LLM-based methods, which rely on prompting frontier LLMs, struggle without additional semantic information. Other than PFNs4BO, these methods heavily rely on the semantic context to generate an accurate understanding of the function space. They therefore fail to meaningfully explore promising regions without this semantic context.

However, with its reliable surrogate, we see that GPOpt outperforms other transformer-based optimizers on these test functions. We also compare GPOpt with the classical and BO optimizers. On these benchmarks, GPOpt is competitive with the best BO methods and outperforms classical optimization over these experiments. This shows that our model performs robust optimization that is competitive with the best BO methods on a variety of black-box problems over a range of dimensions. We also see that GPOpt is consistently a strong performer over the whole step range, with only CMA-ES providing better initial suggestions before tapering off. This suggests that our model is applicable to many different scenarios and problems.

### 4.2. Interpretability

While LLMs are criticized as uninterpretable black boxes, we demonstrate that our model develops a calibrated understanding of the function space, effectively mimicking the predictive capability of a GP. By training on the mean and uncertainty estimates of a GP, our model learns to provide reliable predictions for evaluated points, gradually refining its understanding of the space as sampling progresses.

We validate this alignment by isolating the predictive component of the agent with the goal of answering the following: “If our model is given the exact same history and candidate point as a GP, can it predict the outcome and calibrate its uncertainty with comparable accuracy?” Figure 6 illustrates

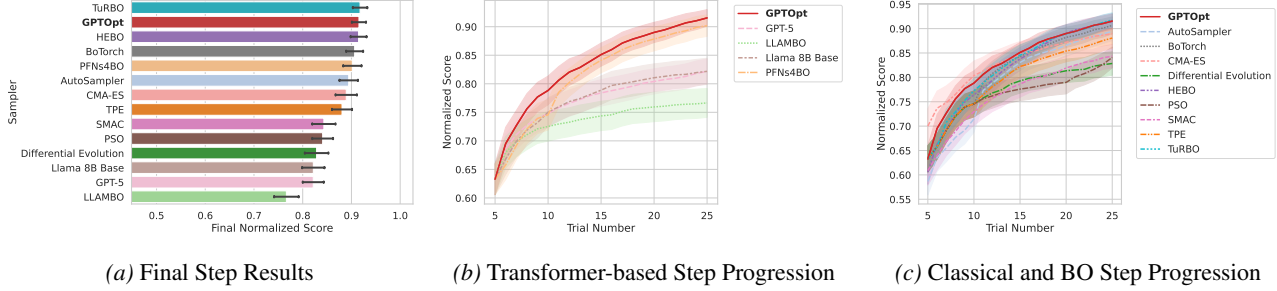


Figure 4. Mean normalized performance with standard error over 5 splits on BBOB 2D, 5D, and 10D test functions. We test over 5 functions from each of the 24 BBOB classes for each dimension, totaling 360 overall functions.

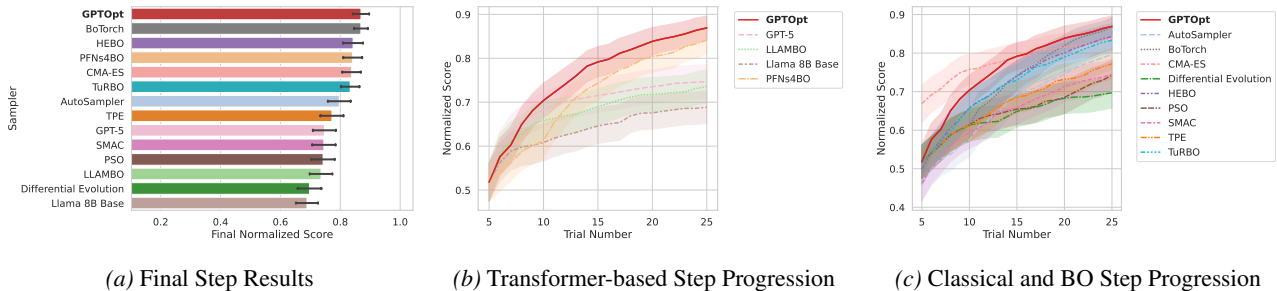


Figure 5. Mean normalized performance with standard error over 5 splits on VLSE 2D, 5D, and 10D test functions. We test over 5 functions from each of the VLSE functions for each dimension, totaling 160 overall functions.

the answer to this question, showing the mean Negative Log Likelihood (NLL) and mean squared error (MSE) of the Base Llama 8B model and GPTOpt compared to the GP baseline given a history of points generated by BO. Both scores are normalized per function and calculated over 25 steps on 100 5D VLSE functions. We see that while the base model can reasonably predict the mean, its unreliable uncertainty estimates result in a huge NLL score. However, the results from GPTOpt indicate our model achieves comparable uncertainty calibration to the GP. This represents a large improvement over the base model, as the model appears to reliably estimate uncertainty within the function space without any semantic priors.

We also assess our model’s ability to characterize the global optimum. We want our model to maintain an accurate surrogate model for high-quality points, particularly the optimal value, as the goal of our model is to reach the optimum. Therefore, we want to show that the model iteratively gains a better understanding of the global optimum as it samples points. We evaluate this by prompting the model to produce mean and standard deviation predictions at the known coordinates of the global optimum after every step as we iterate through a trajectory. Figure 7 presents the normalized MSE of the mean and the mean NLL of these predictions. The results indicate that the model progressively refines its belief as the optimization search converges, as the MSE and NLL statistics decrease with more evaluations. This validates that

our model uses the iterative information and actually uses the updated information provided at each step to inform its predictions.

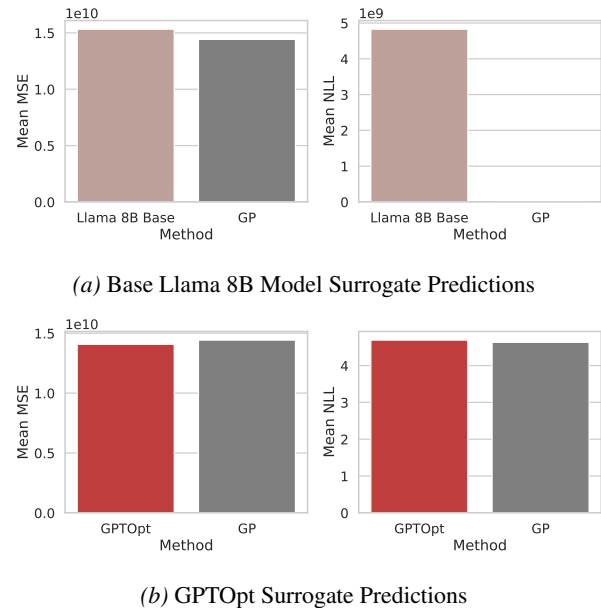


Figure 6. Comparison of surrogate model performance on 5D VLSE functions. The base model has very poor uncertainty calibration, resulting in a large NLL score. However, with its calibrated distribution predictions, GPTOpt achieves similar scores as the GP.

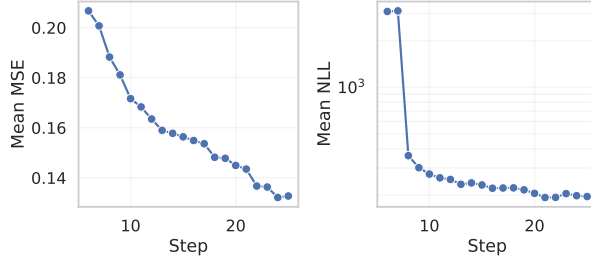


Figure 7. Normalized MSE and Mean Negative Log Likelihood (NLL) of predictions at the global optimum averaged over 100 2D, 5D, and 10D VLSE functions. We evaluate the model’s predicted mean and standard deviation at the ground-truth optimum coordinates after each step. The downward progression indicates the model is learning information about the function space and accurately updating its prediction of the global optimum.

### 4.3. Explainability

To further show the capabilities of an LLM-based model, we provide an example of the explanation capabilities of GPTOpt. Our model can add explanations of why an action was selected, giving a user insight into why the model might be exploring a specific region or exploiting to find a local minimum. The goal here is purely to provide context to a user by providing decision making logic for why they are performing a test. We show an example of this output in Figure 8, where our model generates explanations for a real-world Scikit-learn optimization problem.

```

Assistant: {"Action": {"learning_rate": 0.253468, "subsample": 0.821781}, "Mean": 0.972016, "Std": 0.0022378, "Explanation": "I chose to probe a different learning rate and subsample region to reduce local uncertainty after observing flat or slightly improving performance. The increase in subsample toward mid values targets variance reduction. The learning rate moves slightly upward to check whether boosting capacity improves the objective."}
User: {"Step": 7, "Evaluated Objective": 0.972028}
Assistant: {"Action": {"learning_rate": 0.110572, "subsample": 0.772632}, "Mean": 0.972009, "Std": 0.00180654, "Explanation": "After the evaluation returned slightly worse-than-expected outcomes, I steered subsample modestly downward to maintain model capacity while still lowering variance. The change aims to balance bias and variance by sampling more instances and preventing overfitting. This choice prioritizes learning generalizable patterns indicated by nearby good-performing points."}

```

Figure 8. Example sequence of explanations generated by GPTOpt with real-world context.

### 4.4. Real-World Tests

One of the advantages of an LLM-based optimization is that the LLM can take various input modalities into account. This includes semantic information about specific optimization problems that cannot be provided to traditional optimiz-

ers. We evaluate this using a benchmark that rotates through standard Scikit-Learn (Pedregosa et al., 2011) classification algorithms (Logistic Regression, SVC, MLP, GBM, RF) and datasets (Breast Cancer, Iris, Wine, Digits). This setup challenges optimizers with diverse loss landscapes, including smooth convex surfaces, coupled valleys, local minima, and the discrete, gradient-free plateaus characteristic of tree ensembles, while also allowing for real-world semantic information to be passed to the model. The prompts are given in the same real-world structure used in training.

We compare our model with and without semantic real-world information in Figure 9. We see that incorporating real-world descriptions into the prompt improves model performance on real-world tasks and that performance remains strong when generating explanations. We see this result across the base Llama model and our fine-tuned model, showing that gains with real-world information can be attributed to both fine-tuning and the real-world information. This is important because it shows these gains not just the result of data leakage and the model memorizing good parameters, as our performance is better than the base model with real-world information. Additionally, scaling the base model capability, coupled with our fine-tuning mechanism, may further improve these effects.

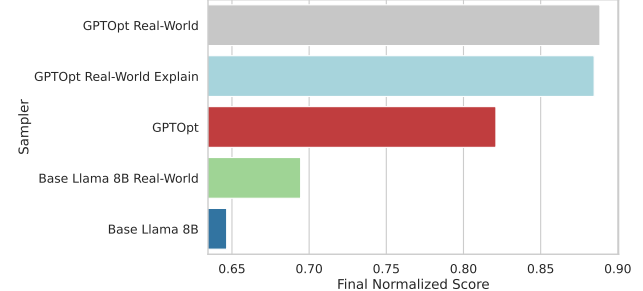


Figure 9. Mean normalized performance on Scikit-Learn test functions. We test over 25 functions, both with and without real-world information.

### 4.5. Trajectory Example

We show three examples of trajectories generated by GPTOpt in Figure 10, showing our model’s ability to explore challenging optimization landscapes. The trajectories begin with 5 random initial samples and show the progression of 20 more steps generated by GPTOpt. We see that the model explores various promising regions and finds the global optimum. These examples are generated on 2D VLSE functions.

### 4.6. Ablations

To determine the best usage of our model, we test which sampling parameters best balance the exploration-exploitation performance. We test various values of  $k$  for the number

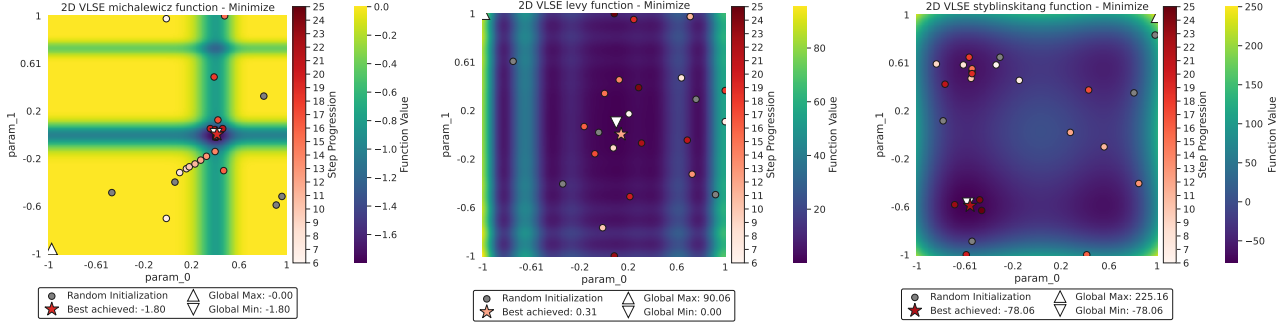
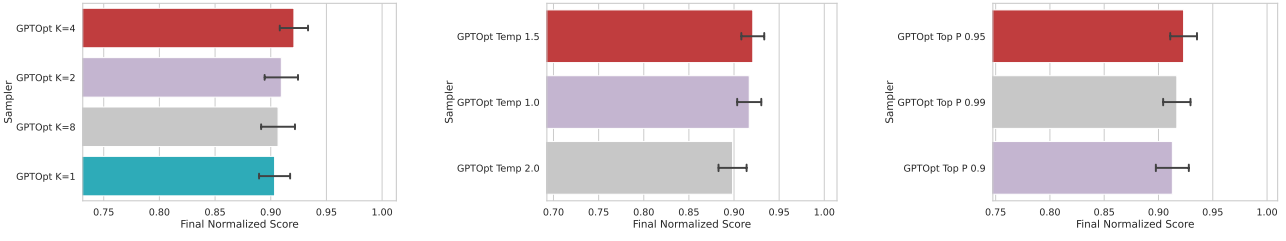


Figure 10. Examples of GPTOpt trajectories on 2D VLSE functions where the goal is to reach the global minimum. We see that the model explores the action space and reaches close to the global minimum on these three challenging landscapes.



(a) Ablation over proposed action count (b) Ablation over sampling temperature (c) Ablation over sampling top-p  
Figure 11. Ablation studies comparing action count, temperature, and top-p. We select our inference parameters from these results.

of actions proposed and selected from by the model at each step in Figure 11 over BBOB test functions. Balancing inference cost with capability is a key challenge for LLM-based methods, where prompting an LLM many times is computationally expensive. We also show results from sampling temperature and top-p selection. We see that the model is consistent over the range of sampling parameters but utilize the best parameter settings as found with these results.

## 5. Conclusions, Limitations, and Future Work

With GPTOpt, we develop a data generation and fine-tuning methodology for LLMs that adds verifiable surrogate modeling capabilities. LLMs have been shown to be powerful tools for black-box optimization problems when combined with semantic context. However, even state-of-the-art LLMs fail to output reliable and robust surrogate model predictions, particularly without additional semantic data. With GPTOpt, we present a data generation and fine-tuning methodology that trains LLMs to produce surrogate model predictions with similar accuracy to GPs, combining the knowledge base of LLMs with more principled optimization strategies. This results in a model that outperforms other transformer-based approaches on benchmark black-box problems and is competitive with state-of-the-art BO methods. We further show that adding real-world semantic information can increase the performance of GPTOpt, showing the promise of

LLMs for solving black-box optimization problems.

Our approach is currently limited to continuous, single-objective optimization in at most 10D, which restricts its applicability to problems involving combinatorial or mixed-integer decision spaces, as well as multi-objective scenarios. Extending the model to tackle these broader categories could significantly enhance its versatility. Additionally, GPTOpt is trained on optimization trajectories generated from Gaussian process-based surrogates, which may encourage behavior aligned with GP-like function classes. While our experiments demonstrate strong generalization across standard benchmarks and real-world tasks, performance on highly nonstationary or adversarial landscapes is an interesting direction for future study.

Future work will focus on expanding the applicability of GPTOpt to a broader range of optimization problems. Specifically, extending our data generation and fine-tuning methodology to support combinatorial, integer, and multi-objective problems would address some of the current limitations in versatility. Additionally, investigating the impact of scaling to larger base models, where increased capacity may enhance the model’s ability to leverage semantic priors for performance gains and generate high-quality, context-aware explanations for real-world tasks. Finally, further scaling of the synthetic training dataset may further improve robustness and generalization across diverse function spaces.

## 6. Acknowledgments

This work is supported by Jane Street and the MIT-IBM Watson AI Lab.

## 7. Impact Statement

This paper presents work whose goal is to advance the field of machine learning. There are many potential societal consequences of our work, none of which we feel must be specifically highlighted here.

## References

Akiba, T., Sano, S., Yanase, T., Ohta, T., and Koyama, M. Optuna: A next-generation hyperparameter optimization framework. In *Proceedings of the 25th ACM SIGKDD International Conference on Knowledge Discovery and Data Mining*, 2019.

Alaa, A. and Schaar, M. Autoprognosis: Automated clinical prognostic modeling via bayesian optimization with structured kernel learning. In *International conference on machine learning*, pp. 139–148. PMLR, 2018.

Ament, S., Daulton, S., Eriksson, D., Balandat, M., and Bakshy, E. Unexpected improvements to expected improvement for bayesian optimization. *Advances in Neural Information Processing Systems*, 36:20577–20612, 2023.

Andrychowicz, M., Denil, M., Gomez, S., Hoffman, M. W., Pfau, D., Schaul, T., Shillingford, B., and De Freitas, N. Learning to learn by gradient descent by gradient descent. *Advances in neural information processing systems*, 29, 2016.

Attia, P. M., Grover, A., Jin, N., Severson, K. A., Markov, T. M., Liao, Y.-H., Chen, M. H., Cheong, B., Perkins, N., Yang, Z., et al. Closed-loop optimization of fast-charging protocols for batteries with machine learning. *Nature*, 578(7795):397–402, 2020.

Balandat, M., Karrer, B., Jiang, D. R., Daulton, S., Letham, B., Wilson, A. G., and Bakshy, E. BoTorch: A Framework for Efficient Monte-Carlo Bayesian Optimization. In *Advances in Neural Information Processing Systems* 33, 2020.

Calandra, R., Seyfarth, A., Peters, J., and Deisenroth, M. P. Bayesian optimization for learning gaits under uncertainty: An experimental comparison on a dynamic bipedal walker. *Annals of Mathematics and Artificial Intelligence*, 76(1):5–23, 2016.

Chaybouti, S., Dos Santos, L., Malherbe, C., and Virmaux, A. Meta-learning of black-box solvers using deep reinforcement learning. In *NeurIPS 2022, MetaLearn Workshop*, 2022.

Chen, Y., Song, X., Lee, C., Wang, Z., Zhang, R., Dohan, D., Kawakami, K., Kochanski, G., Doucet, A., Ranzato, M., et al. Towards learning universal hyperparameter optimizers with transformers. *Advances in Neural Information Processing Systems*, 35:32053–32068, 2022.

Cowen-Rivers, A., Lyu, W., Tutunov, R., Wang, Z., Grosnit, A., Griffiths, R.-R., Maraval, A., Hao, J., Wang, J., Peters, J., and Bou Ammar, H. Hebo: Pushing the limits of sample-efficient hyperparameter optimisation. *Journal of Artificial Intelligence Research*, 74, 07 2022a.

Cowen-Rivers, A. I., Lyu, W., Tutunov, R., Wang, Z., Grosnit, A., Griffiths, R. R., Maraval, A. M., Jianye, H., Wang, J., Peters, J., et al. Hebo: Pushing the limits of sample-efficient hyper-parameter optimisation. *Journal of Artificial Intelligence Research*, 74:1269–1349, 2022b.

Daniel Han, M. H. and team, U. Unsloth, 2023. URL <http://github.com/unslotha/unsloth>.

Dubey, A., Jauhri, A., Pandey, A., Kadian, A., Al-Dahle, A., Letman, A., Mathur, A., Schelten, A., Yang, A., Fan, A., et al. The llama 3 herd of models. *arXiv e-prints*, pp. arXiv–2407, 2024.

Elhara, O., Varelas, K., Nguyen, D., Tusa, T., Brockhoff, D., Hansen, N., and Auger, A. Coco: the large scale black-box optimization benchmarking (bbob-largescale) test suite. *arXiv preprint arXiv:1903.06396*, 2019.

Eriksson, D., Pearce, M., Gardner, J., Turner, R. D., and Poloczek, M. Scalable global optimization via local bayesian optimization. *Advances in neural information processing systems*, 32, 2019.

Erps, T., Foshey, M., Luković, M. K., Shou, W., Goetzke, H. H., Dietsch, H., Stoll, K., von Vacano, B., and Matusik, W. Accelerated discovery of 3d printing materials using data-driven multiobjective optimization. *Science advances*, 7(42):eabf7435, 2021.

Golovin, D., Solnik, B., Moitra, S., Kochanski, G., Karro, J., and Sculley, D. Google vizier: A service for black-box optimization. In *Proceedings of the 23rd ACM SIGKDD international conference on knowledge discovery and data mining*, pp. 1487–1495, 2017.

Griffiths, R.-R. and Hernández-Lobato, J. M. Constrained bayesian optimization for automatic chemical design using variational autoencoders. *Chemical science*, 11(2): 577–586, 2020.

Hansen, N. and Ostermeier, A. Completely derandomized self-adaptation in evolution strategies. *Evolutionary computation*, 9(2):159–195, 2001.

Hansen, N., Müller, S. D., and Koumoutsakos, P. Reducing the time complexity of the derandomized evolution strategy with covariance matrix adaptation (cma-es). *Evolutionary computation*, 11(1):1–18, 2003.

Holland, J. H. *Adaptation in natural and artificial systems: an introductory analysis with applications to biology, control, and artificial intelligence*. MIT press, 1992.

Hu, E. J., Shen, Y., Wallis, P., Allen-Zhu, Z., Li, Y., Wang, S., Wang, L., Chen, W., et al. Lora: Low-rank adaptation of large language models. *ICLR*, 1(2):3, 2022.

Huang, B., Wu, X., Zhou, Y., Wu, J., Feng, L., Cheng, R., and Tan, K. C. Exploring the true potential: Evaluating the black-box optimization capability of large language models. *arXiv preprint arXiv:2404.06290*, 2024.

Hurst, A., Lerer, A., Goucher, A. P., Perelman, A., Ramesh, A., Clark, A., Ostrow, A., Welihinda, A., Hayes, A., Radford, A., et al. Gpt-4o system card. *arXiv preprint arXiv:2410.21276*, 2024.

Jiang, H., Shen, Y., Li, Y., Xu, B., Du, S., Zhang, W., Zhang, C., and Cui, B. Openbox: A python toolkit for generalized black-box optimization. *Journal of Machine Learning Research*, 25(120):1–11, 2024.

Kennedy, J. and Eberhart, R. Particle swarm optimization. In *Proceedings of ICNN'95-international conference on neural networks*, volume 4, pp. 1942–1948. ieee, 1995.

Kirkpatrick, S., Gelatt Jr, C. D., and Vecchi, M. P. Optimization by simulated annealing. *science*, 220(4598):671–680, 1983.

Krishnamoorthy, S., Mashkaria, S. M., and Grover, A. Generative pretraining for black-box optimization. *arXiv preprint arXiv:2206.10786*, 2022.

Lampinen, J. and Storn, R. Differential evolution. In *New optimization techniques in engineering*, pp. 123–166. Springer, 2004.

Lange, R., Tian, Y., and Tang, Y. Large language models as evolution strategies. In *Proceedings of the Genetic and Evolutionary Computation Conference Companion*, pp. 579–582, 2024.

Li, K. and Malik, J. Learning to optimize. *arXiv preprint arXiv:1606.01885*, 2016.

Li, X., Wu, K., Li, Y. B., Zhang, X., Wang, H., and Liu, J. Pretrained optimization model for zero-shot black box optimization. In *The Thirty-eighth Annual Conference on Neural Information Processing Systems*, 2024.

Lindauer, M., Eggensperger, K., Feurer, M., Biedenkapp, A., Deng, D., Benjamins, C., Ruhkopf, T., Sass, R., and Hutter, F. Smac3: A versatile bayesian optimization package for hyperparameter optimization. *Journal of Machine Learning Research*, 23(54):1–9, 2022. URL <http://jmlr.org/papers/v23/21-0888.html>.

Liu, T., Astorga, N., Seedat, N., and van der Schaar, M. Large language models to enhance bayesian optimization. *arXiv preprint arXiv:2402.03921*, 2024.

Maraval, A., Zimmer, M., Grosnit, A., and Bou Ammar, H. End-to-end meta-bayesian optimisation with transformer neural processes. *Advances in Neural Information Processing Systems*, 36, 2024.

Meindl, J., Tian, Y., Cui, T., Thost, V., Hong, Z.-W., Dürholt, J., Chen, J., Matusik, W., and Konaković Luković, M. Zeroshotopt: Towards zero-shot pretrained models for efficient black-box optimization. *arXiv preprint arXiv:2510.03051*, 2025.

Müller, S., Feurer, M., Hollmann, N., and Hutter, F. Pfns4bo: In-context learning for bayesian optimization. In *International Conference on Machine Learning*, pp. 25444–25470. PMLR, 2023.

Ozaki, Y., Watanabe, S., and Yanase, T. OptunaHub: A platform for black-box optimization. *arXiv preprint arXiv:2510.02798*, 2025.

Pedregosa, F., Varoquaux, G., Gramfort, A., Michel, V., Thirion, B., Grisel, O., Blondel, M., Prettenhofer, P., Weiss, R., Dubourg, V., et al. Scikit-learn: Machine learning in python. *the Journal of machine Learning research*, 12:2825–2830, 2011.

Shahriari, B., Swersky, K., Wang, Z., Adams, R. P., and De Freitas, N. Taking the human out of the loop: A review of bayesian optimization. *Proceedings of the IEEE*, 104(1):148–175, 2015.

Shalloo, R., Dann, S., Gruse, J.-N., Underwood, C., Antoine, A., Arran, C., Backhouse, M., Baird, C., Balcazar, M., Bourgeois, N., et al. Automation and control of laser wakefield accelerators using bayesian optimization. *Nature communications*, 11(1):6355, 2020.

Singh, A., Fry, A., Perelman, A., Tart, A., Ganesh, A., El-Kishky, A., McLaughlin, A., Low, A., Ostrow, A., Ananthram, A., et al. Openai gpt-5 system card. *arXiv preprint arXiv:2601.03267*, 2025.

Snoek, J., Larochelle, H., and Adams, R. P. Practical bayesian optimization of machine learning algorithms. *Advances in neural information processing systems*, 25, 2012.

Song, L., Gao, C., Xue, K., Wu, C., Li, D., Hao, J., Zhang, Z., and Qian, C. Reinforced in-context black-box optimization. *arXiv preprint arXiv:2402.17423*, 2024a.

Song, X., Zhang, Q., Lee, C., Fertig, E., Huang, T.-K., Beilenki, L., Kochanski, G., Ariaifar, S., Vasudevan, S., Perel, S., et al. The vizier gaussian process bandit algorithm. *arXiv preprint arXiv:2408.11527*, 2024b.

Surjanovic, S. and Bingham, D. Virtual library of simulation experiments: Test functions and datasets. Retrieved September 20, 2024, from <http://www.sfu.ca/~ssurjano>, 2013.

Tian, Y., Luković, M. K., Erps, T., Foshey, M., and Matusik, W. Autoeo: Automated optimal experiment design platform. *arXiv preprint arXiv:2104.05959*, 2021.

Turner, R., Eriksson, D., McCourt, M., Kiili, J., Laaksonen, E., Xu, Z., and Guyon, I. Bayesian optimization is superior to random search for machine learning hyperparameter tuning: Analysis of the black-box optimization challenge 2020. In *NeurIPS 2020 Competition and Demonstration Track*, pp. 3–26. PMLR, 2021.

Yang, Z., Wang, D., Ge, L., Wang, B., Fu, T., and Li, Y. Reasoning bo: Enhancing bayesian optimization with long-context reasoning power of llms. *arXiv preprint arXiv:2505.12833*, 2025.

## A. Implementation details

### A.1. Data generation

**Synthetic Dataset:** We aim to create realistic and diverse synthetic functions to compile a large-scale dataset for model fine-tuning. To do this, we use Gaussian Processes (GPs) as flexible function generators, which allows for large-scale data collection and realistic landscapes. The intuition here is that GP-based BO methods perform well over a wide variety of function spaces, so by basing our training data on GP functions as well, we hope to learn a policy that also adapts well to other function spaces. To further diversify our training dataset, we vary the scale of input parameters and output parameters to various realistic regimes. For example, we include objectives in  $[0, 100]$  or  $[1, 10]$  and parameters in  $[0, 1]$  or  $[0.0001, 0.1]$ . We randomly generate a large number of random scales to allow for generalization. Our GP-based functions are sampled from a Gaussian process prior defined over the input space. Random covariance kernels are generated by combining base kernels (RBF, Matern, Rational Quadratic, Exponential) using addition and multiplication, with up to three kernels per function. Hyperparameters such as lengthscales and variances are drawn from log-uniform distributions. A fixed set of initial points is sampled, and function values are generated from the corresponding multivariate Gaussian. Evaluations are obtained by conditioning on this prior, yielding smooth but diverse optimization landscapes.

**Augmentations:** We also add further augmentations to the randomly generated GP processes. These augmentations transform smooth GP samples into challenging, realistic landscapes by applying non-linear coordinate warping, introducing discontinuities, and adding complex parameter couplings. The goal of this process is to create a training set that mimics the irregularity of real-world systems (e.g., phase transitions, saturation limits, or discrete configuration spaces). By creating functions with these diverse methods, we provide a base for the model to learn realistic function dynamics across a variety of possible function spaces.

Augmentations include:

- **Nonlinear input warps:** Smooth affine transformations followed by  $\tanh$  nonlinearities to distort the input space density.
- **Hard Discontinuities:** We introduce sharp transitions including staircases (Heaviside jumps), hard gates (switching to flat constant planes past a threshold), mosaics (grid-based piecewise-constant offsets), and hard spots (localized circular bumps or pits).
- **Quantization and Kinks:** To simulate discrete controls or mechanical limits, we apply plateaus (bin snapping/quantization) and kinks (non-differentiable softplus hinges and odd-power bends).
- **High-Order Cross-Couplings:** We explicitly model complex parameter interactions using PolyMix (low-rank quadratic and cubic terms), BiMLP (small MLPs acting on bilinear feature combinations), and Rational Cross-Couplings (singularities and sharp gradients).
- **Manifold Structures:** Specific topological features such as Curvy Tubes (soft manifolds around nonlinear curves), Parity Gates (XOR-like smooth parity functions), Shear Warps (non-separable geometric distortions), and Soft Mixture-of-Experts (combining basis functions via gating networks).
- **Local and Global Texture:** We superimpose micro-textures (localized high-frequency periodic ripples), funnels (ridge-valley conditioning stress), and global trends like linear drifts or quadratic bowls.

Each augmentation is applied with a fixed probability and scaled relative to the natural range of the base function, ensuring meaningful variation without overwhelming the underlying structure.

**BO Data:** We use a variety of global optimization algorithms in each environment to generate expert trajectories. For each of the synthetic functions generated ranging from 2D to 10D, we run BO with 10 acquisition variants. These include LogEI (Ament et al., 2023), Upper Confidence Bound (UCB), Probability of Improvement (PI) acquisition functions with various exploration-exploitation parameters. For LogEI and PI, we adapt the exploration-exploitation level with a range of 3 parameters and for UCB we use a range of 4 parameters. For LogEI and PI, we use  $\xi = [0.0, 0.01, 0.1]$  and for UCB we use  $\kappa = [0.1, 1.0, 2.576, 10.0]$ , which are all standard values for these acquisition functions. These methods are implemented in BoTorch (Balandat et al., 2020). We begin by sampling 5 initial points randomly to initialize each model. We then fit the GP

model to the set of points and use the specified acquisition function to sample a prospective point. After evaluating that point, we refit the model and continue iteratively until 50 total evaluations are reached. We generate trajectories on functions ranging from 2D to 10D. We generate 10,000 synthetic functions per dimension for both GP and augmented GP function spaces, totaling 20,000 functions per dimension, for a total of  $\sim 200,000$  functions.

We generate trajectories using CPU machines, primarily on an Intel Xeon Platinum 8260 system. We find that, although BoTorch supports GPU acceleration, the most cost-efficient manner to generate trajectories is to use parallel CPU processes. However, even with optimizations, running our baseline global optimizers is slow, especially for higher dimensions. Therefore, we total  $\sim 50,000$  vCPU hours for our data generation. We were limited by the number of trajectories we could generate and more data may help improve the model.

## A.2. Prompt Example

We provide an example of a prompt in full in Figure 12. This is a 3D example with 10 total steps. The full dataset contains examples ranging from 2D to 10D and 10 to 50 steps. The prompt begins with a system instruction defining the agent’s role as a black-box optimization assistant and enforcing a strict JSON output format containing the action and predicted mean and standard deviation. The user context then provides a problem description and a history of randomly initialized points. We provide all numbers rounded to 6 significant figures and convert the iterative BO steps into a multi-turn user and assistant conversation. The interaction follows in a turn-based manner where the assistant proposes a new configuration, which is the action proposed by BO and the GP’s predicted mean and standard deviation, and the user returns the evaluated objective value, repeating until the evaluation budget is exhausted.

## A.3. Real-world Context and Explanations

To further expand the capabilities of our model, we augment our synthetic dataset with two types of LLM-generated descriptions. First, we generate descriptions of real-world problems, including descriptions of the overall problem, the parameters to optimize, and the evaluation metric. This associates the model with diverse and realistic descriptions that the model can use as semantic information for real-world experiments. We generate 10,000 real-world tasks ranging in dimension from 2D to 10D, with descriptions for the problem, parameters, and evaluation using GPT-5 Mini (Singh et al., 2025). Additionally, we augment a portion of our dataset with LLM-generated explanations for each action selection. We generate these using prompts to GPT-5 Mini for 10,000 prompt examples, half of which contain the real-world context generated above. To do this, we include the BO trajectory in the prompt, asking the LLM to explain the decision-making process behind each step given the available information. In total, the real-world context or explanations are included for around 1% of our overall dataset, containing 20,000 examples in total.

## A.4. Training

Our full dataset contains 10 trajectories generated for each of the  $\sim 200,000$  total functions. We compile a training dataset by selecting the best performing trajectories at various step counts (i.e., the first 25 steps of a 50 step trajectory). We take the best trajectory after 10, 25, and 50 steps as the training data for our model. Therefore, the model learns to act like the best acquisition functions do around various step counts. We use data augmentation to further expand this dataset. We augment by swapping axes, flipping the action space, and randomizing the order of the initial points to provide additional training data. This augmentation greatly expands the trajectory space, particularly for higher dimensions. This results in a total of around 2 million trajectories included in the dataset. We further add the LLM generated real-world problems and LLM-generated explanations, as detailed above.

We use the Llama 3.1 family of models as our base model (Dubey et al., 2024). Specifically, we use the 8B Instruct model for our experiments. This is a text-only LLM that provides a model with reasonable capabilities, but is manageable to fine-tune within our compute budget. Expanding the size of the base model is a possibility for further improvement. We fine-tune the model using low-rank adaptation (LoRA) (Hu et al., 2022) with Unslloth (Daniel Han & team, 2023). This provides a fast and efficient framework for fine-tuning LLMs, which allows us to train models within our computational limits. We begin by compiling our dataset of conversational trajectories and complete a training run on the full dataset. We then utilize this trained model for all experiments.

We use the hyperparameters shown in Table 1 to fine-tune the model, which are informed by best practices from Unslloth. These trajectories are inputted in the text form shown in Figure 12 and trained via supervised next-token prediction on the

**System:** You are a black-box optimization assistant. Your goal is to iteratively select new points to maximize the objective within 10 total evaluations. You must output the raw parameter values within the specified ranges as well as a predicted mean and standard deviation for the selected point.

Output exactly ONE valid JSON object containing the "Action", "Mean", and "Std", with no surrounding text.

**User:** Problem description:  
This problem is a synthetic 3D black-box optimization problem.

The JSON must have exactly these keys:

```
{"Action": {"param_0": <float in [0, 1]>, "param_1": <float in [0, 1]>, "param_2": <float in [0.000207408, 0.132301]>}, "Mean": <float>, "Std": <float>}
```

We have collected 5 random initial points:

```
{"Step": 1, "Action": {"param_0": 0.406795, "param_1": 0.31867, "param_2": 0.00536228}, "Evaluated Objective": 660479}
{"Step": 2, "Action": {"param_0": 0.835194, "param_1": 0.12087, "param_2": 0.107585}, "Evaluated Objective": 643520}
{"Step": 3, "Action": {"param_0": 0.52533, "param_1": 0.903538, "param_2": 0.0691058}, "Evaluated Objective": 628667}
{"Step": 4, "Action": {"param_0": 0.445769, "param_1": 0.746866, "param_2": 0.0449474}, "Evaluated Objective": 638898}
{"Step": 5, "Action": {"param_0": 0.353633, "param_1": 0.602819, "param_2": 0.112898}, "Evaluated Objective": 650711}
```

Based on the history, iteratively generate the next configuration to maximize the objective. You have 5 evaluations left.

**Assistant:** {"Action": {"param\_0": 0.17325, "param\_1": 0.322586, "param\_2": 0.000207408}, "Mean": 658314, "Std": 7094.09}

**User:** {"Step": 6, "Evaluated Objective": 651697}

**Assistant:** {"Action": {"param\_0": 0.423048, "param\_1": 0.274942, "param\_2": 0.132301}, "Mean": 658769, "Std": 5029.98}

**User:** {"Step": 7, "Evaluated Objective": 648513}

**Assistant:** {"Action": {"param\_0": 0.587375, "param\_1": 0.150438, "param\_2": 0.000207408}, "Mean": 658497, "Std": 5994}

**User:** {"Step": 8, "Evaluated Objective": 677102}

**Assistant:** {"Action": {"param\_0": 0.827033, "param\_1": 0.0875877, "param\_2": 0.000207408}, "Mean": 676478, "Std": 6696.23}

**User:** {"Step": 9, "Evaluated Objective": 639092}

**Assistant:** {"Action": {"param\_0": 0.546222, "param\_1": 0.00189189, "param\_2": 0.000207408}, "Mean": 673690, "Std": 7363.99}

**User:** {"Step": 10, "Evaluated Objective": 664354}

---

*Figure 12.* Example interaction loop. The prompts are provided in full here for this example of a 3D optimization problem with 10 total evaluations allowed. The full dataset contains 2 million examples like this ranging from 2D to 10D and containing between 10 and 50 total evaluations.

assistant portions only. This training takes around 7 days on two NVIDIA H200 GPUs. Further training was limited by computational budgets.

## A.5. Inference

During inference, we leverage the probabilistic nature of the fine-tuned LLM. At each optimization step  $t$ , we prompt the model  $k$  times in parallel with the same interaction history  $\mathcal{D}_t$ . Due to the stochastic sampling of the LLM, this yields a set of  $k$  candidate responses, where each response  $j \in \{1, \dots, k\}$  consists of a proposed action  $\mathbf{x}^{(j)}$  and the associated surrogate model predictions  $\mu^{(j)}$  and  $\sigma^{(j)}$ .

To select the final action  $\mathbf{x}_{t+1}$  for evaluation, we calculate the Expected Improvement (EI) for each of the  $k$  candidates based on their self-predicted distributions  $\mathcal{N}(\mu^{(j)}, \sigma^{(j)2})$  relative to the best value observed so far,  $y_t^* = \text{opt}_{(\mathbf{x}, y) \in \mathcal{D}_t} y$ . Here,  $\text{opt}$  refers to max for maximization and min for minimization tasks. The improvement  $I$  is defined as  $\max(0, y - y_t^*)$  for

Table 1. Hyperparameters for model training.

Hyperparameter	Value
Base Model	Llama 3.1 8B Instruct
Learning Rate	$1 \times 10^{-4}$ with cosine scaling
Weight Decay	0.01
Batch Size	128 trajectories
LoRA R	128
LoRA Alpha	128
Bias	None
Dropout	0.0
Precision	BF16
Epochs	1

maximization and  $\max(0, y_t^* - y)$  for minimization. We select the candidate that maximizes this expected improvement:

$$\mathbf{x}_{t+1} = \mathbf{x}^{(j^*)} \quad \text{where} \quad j^* = \arg \max_j \text{EI}(\mu^{(j)}, \sigma^{(j)}, y_t^*)$$

This selection mechanism allows the model to filter its own proposals, giving it an exploration-exploitation balance. For all experiments, we set the number of generations  $k = 4$ . We utilize a high sampling temperature of 1.5 and a top-p value of 0.95, as determined through ablation studies.

#### A.6. Compute Comparison

While the training of GPTOpt takes significant compute, including during the data generation phase, we target high-cost evaluation domains that heavily negate this additional cost. For our regime of ultra-low evaluation budgets, it is assumed that the cost of each evaluation is very high and the cost of the optimization method is negligible. However, we also have advantages in compute cost compared to other LLM-based methods including LLAMBO (Liu et al., 2024), which utilizes frontier LLMs via an API. We utilize a fine-tune of an 8B parameter LLM, which can run on many systems at fairly low cost. Overall, GPTOpt does utilize more compute than a BO-based system, but in a regime where sample efficiency is most important, this difference is negated.

## B. Evaluations

We provide further detail into the evaluation strategy used for both benchmarks and baselines in our experiments. We aim to test over a broad range of benchmarks and state-of-the-art baselines.

### B.1. Benchmarks

**BBOB (Elhara et al., 2019):** The Black-Box Optimization Benchmarking suite was developed as part of the COCO (Comparing Continuous Optimizers) platform to provide a rigorous and standardized environment for evaluating continuous, unconstrained optimization algorithms. BBOB includes 24 benchmark functions that represent a wide range of challenges encountered in real-world optimization, such as separability, multimodality, ill-conditioning, and non-convexity. Each function is parameterized with randomized shifts, scalings, and rotations to prevent algorithms from overfitting to specific patterns. The suite was carefully designed through mathematical constructions and transformations of base functions to create controlled yet diverse test cases. It supports varying dimensions and is widely used in the black-box optimization community.

**VLSE (Surjanovic & Bingham, 2013):** The Virtual Library of Simulation Experiments is a benchmark suite aimed at simulating real-world optimization problems where the objective function is defined by computational simulations rather than closed-form expressions. We use the optimization test problems from this set, which contain different fixed problems for each dimension.

**Real-World Scikit-Learn Tests (Pedregosa et al., 2011):** We develop a benchmark suite of real-world problems by running Scikit-Learn classification problems on standard Scikit-Learn datasets. These classification algorithms (Logistic

Regression, SVC, MLP, GBM/RF) and datasets (Breast Cancer, Iris, Wine, Digits) represent real-world tasks that are similar to ones real users may need to solve. This setup challenges optimizers with diverse loss landscapes, including smooth convex surfaces, coupled valleys, local minima, and the discrete, gradient-free plateaus characteristic of tree ensembles, while also allowing for real-world semantic information to be passed to the model. This information is passed to the model in the specific structure that was used in training.

## B.2. Baselines

The majority of our baselines come from Optuna (Akiba et al., 2019) and OptunaHub (Ozaki et al., 2025), which provide black-box optimization environments and sampler implementations.

### B.2.1. CLASSICAL & EVOLUTIONARY APPROACHES

**CMA-ES (Covariance Matrix Adaptation Evolution Strategy)** (Hansen et al., 2003) An evolutionary algorithm designed for non-linear, non-convex optimization problems. It adapts a covariance matrix to represent the search distribution, making it particularly effective for continuous domain problems with complex landscapes.

**PSO (Particle Swarm Optimization)** (Kennedy & Eberhart, 1995) A stochastic optimization technique based on swarm intelligence. It optimizes a problem by iteratively trying to improve candidate solutions by moving them around the search space according to the particle's position and velocity.

**Differential Evolution** (Lampinen & Storn, 2004) A population-based optimization algorithm that iteratively improves a candidate solution. It uses vector differences between randomly selected population members to perturb existing vectors, creating a mutation mechanism that drives the search.

### B.2.2. BAYESIAN OPTIMIZATION (BO)

**TPE (Tree-structured Parzen Estimator)** A Bayesian Optimization approach that fits multiple Gaussian mixture models to sets of the best parameters and all parameters, calculating the ratio between the two to select the next point.

**HEBO (Heteroscedastic Evolutionary Bayesian Optimization)** (Cowen-Rivers et al., 2022b) A state-of-the-art BO method that combines evolutionary algorithms with surrogate modeling. It is designed to handle heteroscedasticity and uses non-linear transformations to improve robustness in complex search spaces.

**TuRBO** (Eriksson et al., 2019) TuRBO is a BO method that fits GPs to specified trust regions around points of interest. This reduces complexity, particularly in high-dimensions and has proven to be a robust global optimizer.

**SMAC (Sequential Model-Based Algorithm Configuration)** (Lindauer et al., 2022) A versatile BO method often used for hyperparameter tuning. It defaults to using random forests as the surrogate model, allowing it to handle discrete and conditional parameters effectively.

**BoTorch (Balandat et al., 2020)** A library built on PyTorch that provides Bayesian Optimization primitives. In this context, it represents BO using Gaussian Processes and a LogEI acquisition function. We use their default model and acquisition for our experiments, but many different parameterizations are possible here.

**AutoSampler** An Optuna (Akiba et al., 2019) mechanism that automatically selects the most appropriate sampling strategy, switching between TPE for independent parameters and CMA-ES for correlated parameters based on the provided search space configuration.

## B.3. Transformer-Based & Learned Optimization

**LLAMBO (Large Language Model Bayesian Optimization)** (Liu et al., 2024) A method that leverages pre-trained Large Language Models (LLMs) to enhance Bayesian Optimization using frontier models. The OptunaHub implementation defaults to using GPT-4o mini (Hurst et al., 2024) as the default model. It heavily utilizes the LLM's world knowledge to inform the surrogate modeling process.

**PFNs4BO (Prior-Data Fitted Networks for BO)** (Müller et al., 2023) A transformer-based approach utilizing prior-data fitted networks where a neural network is pre-trained on a massive dataset of synthetic functions. It acts as a surrogate model that can perform Bayesian Optimization inference in a single forward pass, bypassing the need for traditional GP fitting. We use their pre-trained HEBO plus model, as prescribed in their example code.

#### B.4. LLM Baselines

**OpenAI GPT-5 (Singh et al., 2025) & Llama 3.1 8B Instruct (Dubey et al., 2024)** These general-purpose Large Language Models are used as zero-shot optimization agents. Without specific fine-tuning, these models rely on in-context learning and pre-trained reasoning capabilities to suggest parameters based on the prompt structure used for the fine-tuned model. We test these using the same input structure and information as GPTOpt. We aim to show that base LLMs are not capable of complex black-box optimization without additional semantic data and require a more principled data source, such as data from a Gaussian process, to accurately understand and optimize a function space. Therefore, we compare with a state-of-the-art LLM in GPT-5 and demonstrate the effectiveness of our fine-tuning by comparing with Llama 3.1 8B Instruct.

### C. Additional Results

We provide further results showing the performance of GPTOpt under different conditions and metrics. We aim to show GPTOpt is a flexible method and provides robust results across these different experimental settings.

### D. Alternative Evaluation Counts

We show the performance of GPTOpt with different evaluation counts, including 10 total steps, 25 total steps, and 50 total steps on BBOB 2D and 5D functions in Figures 13, 14, and 15, respectively. We see that the performance of GPTOpt decreases for 50 step trajectories, but is still competitive with state-of-the-art methods. However, this remains an area of future research and further improvements for larger budget situations would be beneficial. These evaluations contain only the traditional and BO-based methods due to the required API usage of other LLM-based methods.

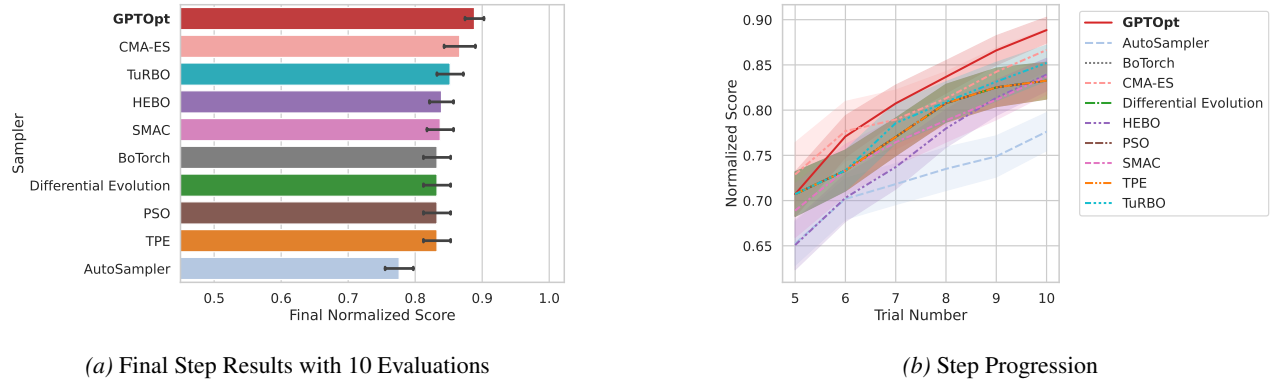


Figure 13. Mean normalized performance with 10 total evaluations with standard error over 5 splits on BBOB 2D and 5D test functions. We test over 5 functions from each of the BBOB functions for each dimension, totaling 240 overall functions.

### E. Win-rate

We show the win rate of GPTOpt against all baselines on BBOB and VLSE test suites for 2D, 5D, and 10D functions with 25 total evaluations in Figure 16. We calculate win-rate by comparing the best objective value achieved by GPTOpt against each other method for every function and calculating the rate at which GPTOpt is better, giving a score of 0.5 when they are equal. We see that GPTOpt beats transformer-based methods and is competitive with state-of-the-art BO methods over both datasets. This provides another important metric justifying the reliability of GPTOpt performance.

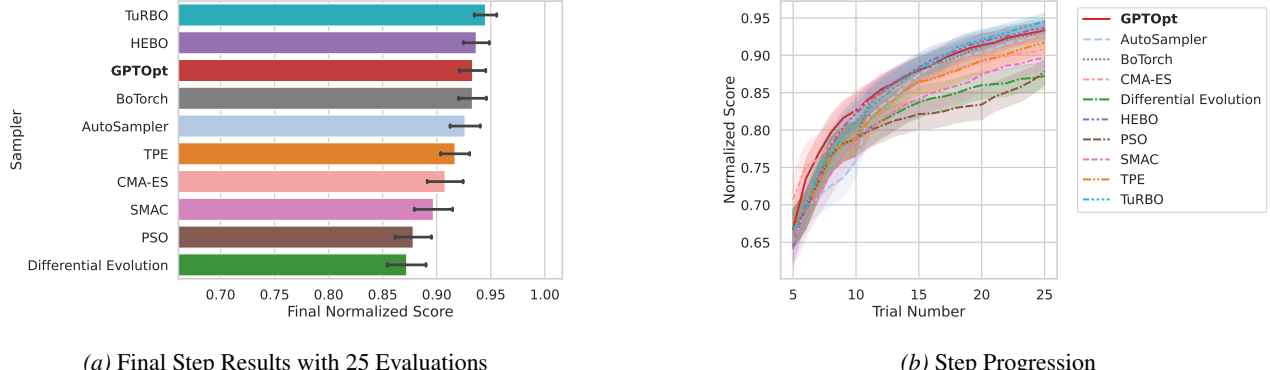


Figure 14. Mean normalized performance with 25 total evaluations with standard error over 5 splits on BBOB 2D and 5D test functions. We test over 5 functions from each of the BBOB functions for each dimension, totaling 240 overall functions.

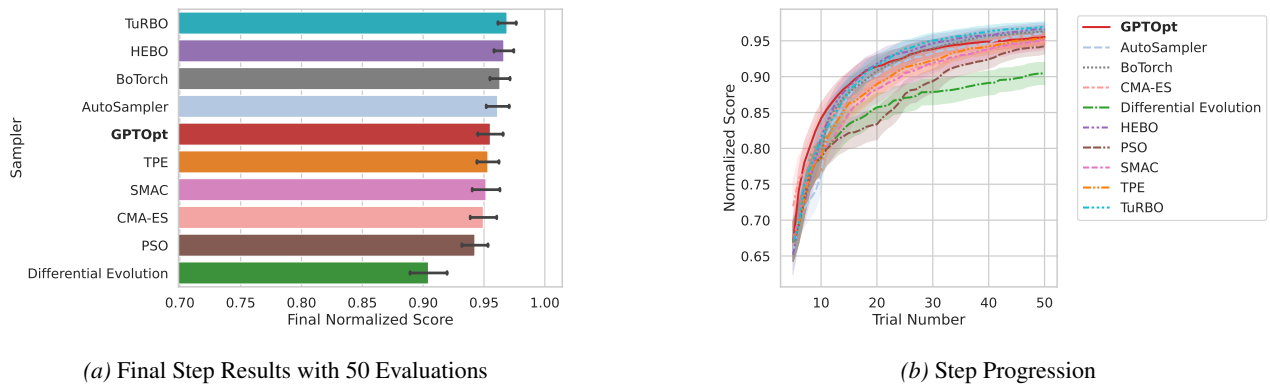


Figure 15. Mean normalized performance with 50 total evaluations with standard error over 5 splits on BBOB 2D and 5D test functions. We test over 5 functions from each of the BBOB functions for each dimension, totaling 240 overall functions.

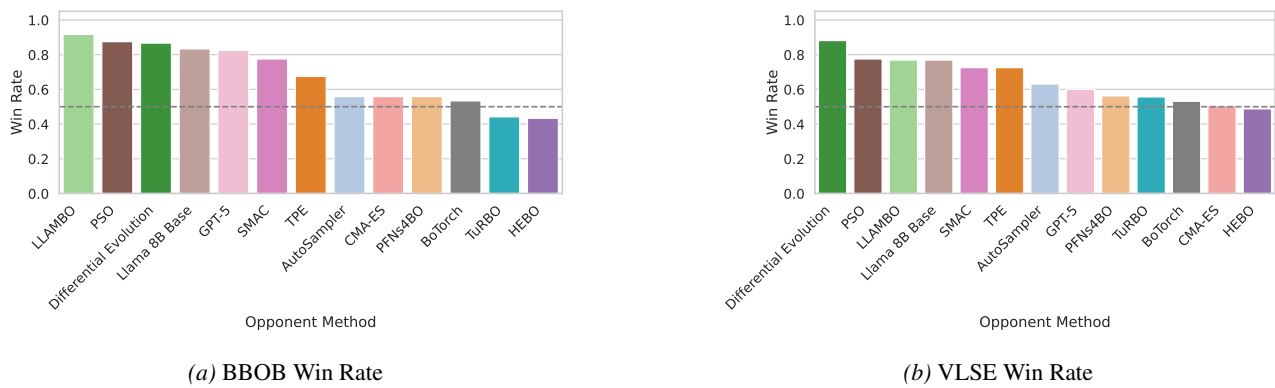


Figure 16. Win rate of GPTOpt compared to baselines on 2D, 5D, and 10D BBOB and VLSE functions. We test over 5 functions from each of the BBOB and VLSE functions for each dimension, totaling 360 overall functions for BBOB and 160 functions for VLSE.